REPORT DOCUMENTATION PAGE

OMB No. 0704-0188

1. REPORT DATE (DD-MM-YYYY)	2. REPORT TYPE	3. DATES COVERED (From - To)
03/31/07	Final	03/01/04 thru 12/31/06

4. TITLE AND SUBTITLE
New Generation Photonics Materials: Design, Development, Characterization, and Applications.

5a. CONTRACT NUMBER

5b. GRANT NUMBER
FA9550-04-1-0158

5c. PROGRAM ELEMENT NUMBER

6. AUTHOR(S)
Prasad, Paras N.
He, Guang S.

5d. PROJECT NUMBER

5e. TASK NUMBER

5f. WORK UNIT NUMBER

7. PERFORMING ORGANIZATION NAME(S) AND ADDRESS(ES)
University at Buffalo
Natural Science Complex
North Campus
Amherst, NY 14260

8. PERFORMING ORGANIZATION REPORT NUMBER

9. SPONSORING / MONITORING AGENCY NAME(S) AND ADDRESS(ES)
Research Foundation of SUNY
P.O. Box 9
Albany, NY 12201-0009
Dr Charles Lee NA

10. SPONSOR/MONITOR'S ACRONYM(S)

11. SPONSOR/MONITOR'S REPORT NUMBER(S)

AFRL-SR-AR-TR-07-0181

12. DISTRIBUTION / AVAILABILITY STATEMENT
Approved for public release,
distribution unlimited

13. SUPPLEMENTARY NOTES

14. ABSTRACT
Significant research achievements have been accomplished in development of multi-photon active materials and applications as well as of novel nanocomposites materials for opto-electronic technology. The specific research progress achieved by this grant supportcan be summarized as follows. (I) Nonlinear optical limiting and stabilization of 1064 nm laser pulses using a novel two-photon absorbing liquid dye salt system. The major advantage of using a neat liquid dye salt as the two-photon absorbing medium is that the effective molar concentration can be increased by two orders of magnitude and it can withstand much higher input laser energy and intensity. (II) A new-type stimulated Rayleigh-Bragg scattering generated in a novel two-photon absorbing dye solution. It is a two-photon excitation enhanced backward stimulated Rayleigh scattering in a nonlinearly absorbing dye solution. This stimulated scattering shows no frequency shift and therefore is different from most of other known stimulated scattering processes. The principle of this effect can be highly useful for optical phase-conjugation technique and optical power limiting applications. (III) Synthesis, two- and three-photon absorption, and optical limiting properties of fluorene containing ferrocene derivatives and novel dendritic structures. These newly designed and synthesized systems have provided a considerably improved two- and three-photon absorption cross-section values, and demonstrated good optical power limiting behavior in fs-regime for both 775-nm and 1300 nm wavelengths. (IV) Efficient photoconductivity and photorefractivity at infrared wavelengths in hybrid nanocomposites: (a) high photoconductivity at optical communication wavelengths in solution-processed hybrid organic:inorganic nanocomposites consisting of infra-red active quantum dots as photosensitizers; (b) large enhancement of photoconductivity in the nanocomposite by incoprporating organic transistor molecule pentacene; and (c) polymer-quantum dot nanocomposite photorefractive devices operating at 1340 and 1550 nm optical communication wavelengths.

15. SUBJECT TERMS
Multi-photon materials, Quantum Dots, Nanocomposites, Photorefractivity, Electro-Optics

16. SECURITY CLASSIFICATION OF:			17. LIMITATION OF ABSTRACT	18. NUMBER OF PAGES	19a. NAME OF RESPONSIBLE PERSON
a. REPORT	b. ABSTRACT	c. THIS PAGE			19b. TELEPHONE NUMBER (include area code)

Standard Form 298 (Rev. 8-98)
Prescribed by ANSI Std. Z39.18

Final Report

(3/31/2007)

Prime Grant: FA9550-04-1-0158

RF account number: 32154-1-1039014

New Generation Photonics Materials: Design, Development, Characterization and Applications

Submitted by Prof. Paras N. Prasad

Institute for Lasers, Photonics and Biophotonics

State University of New York at Buffalo

Contents

Part I. Novel multi-photon absorbing materials for optical power limiting and stabilization applications

1-1. Degenerate nonlinear absorption and optical power limiting properties of asymmetrically substituted stilbenoid chromophores

Two-photon absorption (2PA) spectra (650–1000 nm) of a series of model chromophores were measured *via* a newly developed nonlinear absorption spectral technique based on a single and powerful femtosecond white-light continuum beam. The experimental results suggested that when either an electron-donor or an electron-acceptor was attached to a *trans*-stilbene at a *para*-position, an enhancement in molecular two-photon absorptivity was observed in both cases, particularly in the 650–800 nm region. However, the push–pull chromophores with both the donor and acceptor groups showed larger overall two-photon absorption cross-sections within the studied spectral region as compared to their mono-substituted analogues. The combined results of the solvent effect and the ^{1}H-NMR studies indicated that stronger acceptors produce a more efficient intramolecular charge transfer character upon excitation, leading to increased molecular two-photon responses in this model-compound set. A fairly good 2PA based optical power limiting behavior from one of the model chromophores is also demonstrated.

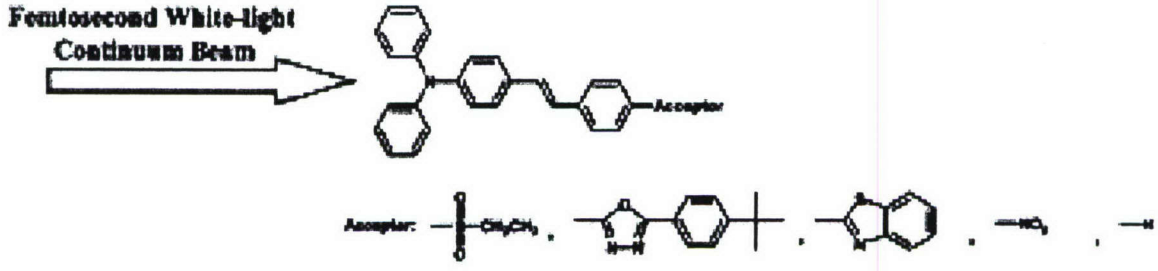

Fig. 1 Chemical structures of the selected stilbenoid chromophores.

(Lin, Tzu-Chau; He, Guang S.; Prasad, Paras N.; Tan, Loon-Seng. Journal of Materials Chemistry (2004), **14**, 982-991.)

1-2. Novel two-photon absorbing, 1,10-phenanthroline containing p-conjugated chromophores and their nickel(II) chelated complexes with quenched emissions

Novel 1,10-phenanthroline containing p-conjugated chromophores with various electron donors were synthesized and characterized together with their corresponding nickel(II) chelated complexes. The linear absorption maxima for these chromophores could be tuned from 357 nm to 415 nm by using different electron donors. The 1,10-phenanthroline containing p-conjugated chromophores exhibit strong fluorescence in solution upon one-photon or two-photon excitation. The fluorescence of these chromophores can be quenched or partially quenched by some metal ions due to an excellent metal-ion chelating ability of the 1,10-phenanthroline backbone. The nickel(II) chelating complexes show quenched emission, both in dilute and concentrated solutions, compared to their metal ion-free chromophores. Their two-photon absorption (2PA) spectra are obtained by using a newly developed multi-photon spectroscopic technique which utilizes a single strong femtosecond white-light continuum generation beam. The two-photon absorption spectra show that the 2PA band for these compounds can be tuned by choosing different electron donors. The maximum 2PA cross-section σ_2 values for the three metal ion-free chromophores are variable from 0.58 to 2.26×10^{-20}cm^4/GW (±15 %). The metal ion-free chromophore containing dihexylamino groups has a larger TPA cross-section σ_2 value compared to the chromophores containing alkyloxy groups or alkylthio groups. When the metal ion-free chromophores coordinate with nickel(II) ion, the resulting complexes do not lose their excellent two-photon absorbing ability. The nickel(II) chelated complexes display red-shifted two-photon absorption bands compared to their metal ion-free chromophores.

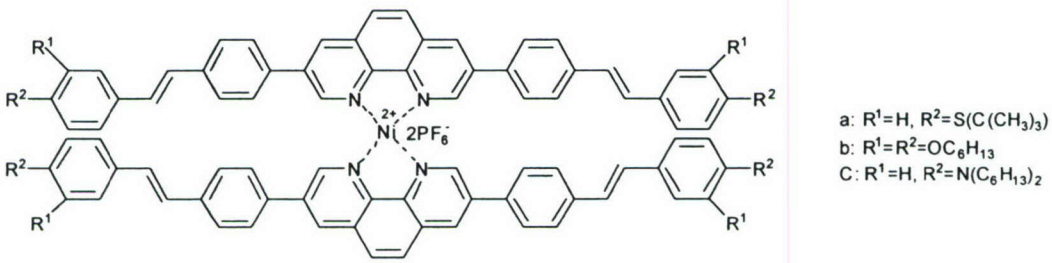

Fig. 2 Chemical structures for nickel (II) chelated 1,10-phenanthroline containing chromophores.
(Qingdong Zheng, Guang S He, and Paras N. Prasad. Journal of Materials Chemistry, 2005, **15**, 579-587)

1-3. Synthesis, two-photon absorption and three-photon absorption properties of novel fluorene containing ferrocene derivatives

We have synthesized and characterized two novel fluorene containing ferrocene derivatives. The combination of fluorine and ferrocene has resulted in compounds with large 2PA and 3PA in the IR region as well as excellent thermal stability up to 453 °C. The results show that ferrocene complexes are excellent candidates for multi-photon absorbing materials.

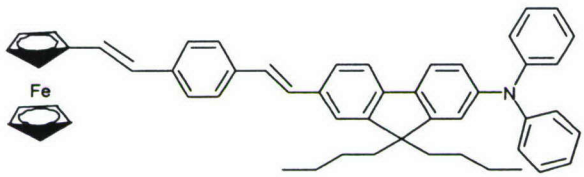

1

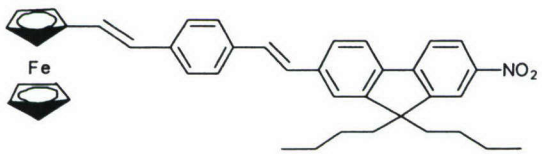

2

Fig. 3 Molecular structures of fluorene containing ferrocene derivatives.

(Qingdong Zheng, Guang S. He, Changgui Lu, Paras N. Prasad, Journal of Materials Chemistry, 2005, **15**, 3488-3493)

The synthesis and characterization of two novel fluorene containing ferrocene derivatives (**1** and **2**) were reported. The two-photon absorption spectra and three-photon absorption cross-section values in IR region for these two chromophores were studied. Together with their thermal stabilities, their linear absorption and emission properties were also investigated. The results show that the ferrocene derivatives have large two-photon and three-photon absorption in IR region as well as excellent thermal stabilities. Three-photon absorption based optical limiting properties of these two ferrocene derivatives were investigated by using sub-picosecond IR laser pulses.

1–4. Synthesis and applications of novel π-conjugated dendritic nanosized chromophores with enhanced two- and three-photon absorption

A novel π-conjugated dendritic nanosized chromophore, 1,3,5-tris(7,12-bis(2-{4-[2-(7-diphenylamino-9,9-dibutyl-*9H*-fluoren-2-yl)-vinyl]-phenyl}-vinyl)-5,5,10,10,15,15-hexabutyl-

10,15-dihydro-5*H*-diindeno[1,2-*a*;1',2'-*c*]fluoren-2-yl)-benzene (**3**), was synthesized and characterized, together with its corresponding one- and three-branched units. Two-photon absorption (2PA) spectra for these chromophores were measured by the nonlinear transmission spectral technique which utilizes a femtosecond white-light continuum. The TPA peak value for the dendritic chromophore is 5.47×10^{-20} cm^4/GW, 15.6 times larger than that for the one-branched dipolar chromophore (0.35×10^{-20} cm^4/GW), [9,9-dibutyl-7-(2-{4-[2-(9,9-dibutyl-9*H*-fluoren-2-yl)-vinyl]-phenyl}-vinyl)-9*H*-fluoren-2-yl]-diphenylamine (**1**). The three-branched chromophore, 2,7,12-tris(2-{4-[2-(9,9-dibutyl-7-diphenylamino-9*H*-fluoren-2-yl)-vinyl]-phenyl}-vinyl)-5,5,10,10,15,15-hexabutyl-10,15-dihydro-5H-diindeno[1,2-a;1',2'-c]fluorene (**2**) has a TPA peak value of 2.28×10^{-20} cm^4/GW, 6.5 times as large as that for compound **1**.

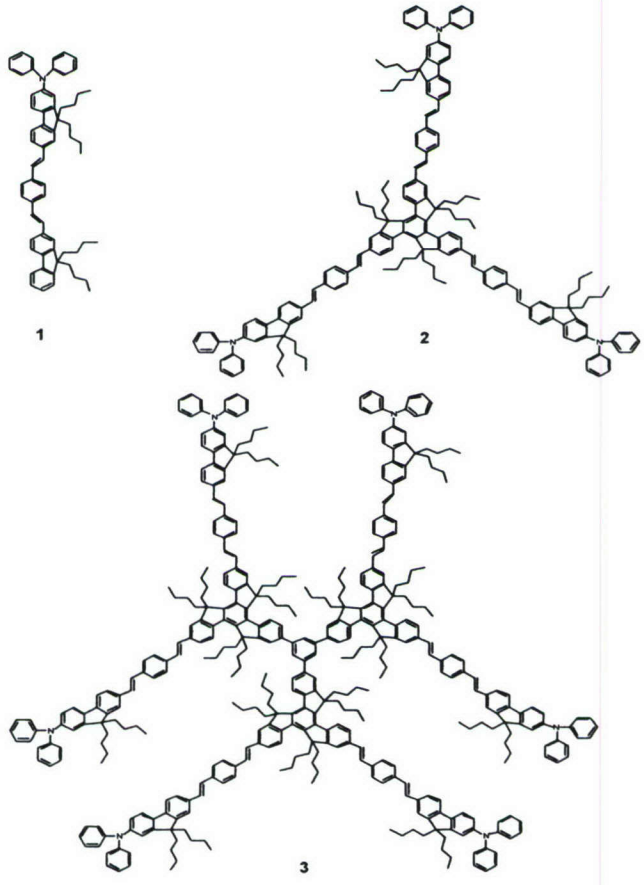

Fig. 4 Molecular structures of chromophores **1-3.**

(Qingdong Zheng, Guang S. He, Paras N. Prasad, Chemistry of Materials, 2005, 17(24), 6004-6011)

The enhanced two-photon absorption found in these two multibranched chromophores is attributed to the fact that the dendritic or the three-branched chromophore has both an extended π -conjugated system and an increased intramolecular charge redistribution compared to the one-branched chromophore. With use of comparable structure unit based concentrations, the two-photon excited (2PE) fluorescence intensity for this dendritic chromophore (0.0033 M solution) was found to be enhanced by a factor of 2.9 compared to that for chromophore **1** (0.02 M solution), which would offer a major advantage in TPE fluorescence related applications.

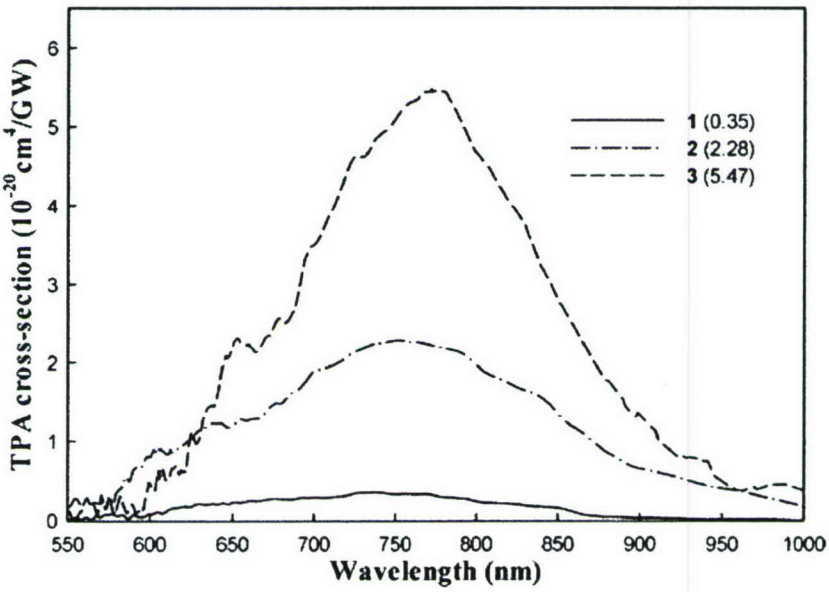

Fig. 5 Two-photon absorption spectra for chromophores 1-3

The measured 2PA spectra for these chromophores are shown in Fig. 5. As shown in Fig. 5, the dendritic chromophore **3** has extremely large two-photon absorption around 800 nm in a femtosecond regime (5.47×10^{-20} cm^4/GW). Hence, one may find in Fig. 5 that the 2PA cross-section peak value increases by a factor of 6.5 and 15.6 when going from **1**, to **2** and **3**, respectively. Considering that compounds **1**, **2**, and **3** have one, three, and six branches, respectively, there is a 160% TPA enhancement on going from **1** to **3**, a 117% enhancement on going from **1** to **2**, and a 20% enhancement on going from **2** to **3**. This dramatic enhancement in TPA can be attributed to the extended π-conjugated system in compounds **2** and **3** as we expected. At the same time, compounds **2** and **3** show red-shifted two-photon absorption bands compared to compound **1**, due to their extended π-conjugated systems.

In this study, cooperative enhancement of three-photon absorption (3PA) cross section was also observed in going from a one-branched (1) to a three-branched (2) and then to a dendritic structure (3). Experimentally, we observe a 72 % enhanced 3PA cross-section value in going from the one-branched chromophore to the dendritic chromophore, and a 49 % enhanced 3PA cross-section value in going from the one-branched chromophore to the three-branched chromophore, when the 3PA cross-section values are normalized per structure unit. Quantum chemical calculation for the one- and three-branched structures, using the cubic response (CR) theory applied to a single determinant SCF (SCF) ref. state, also predicts such an enhancement. Two-dimensional-delocalization, resulting in extended charge-transfer network in the case of the multibranched structures, is the main cause of the cooperative enhancement. Owing to the increased 3PA cross-section value for the dendritic chromophore, improved optical limiting performance at an optical communication wavelength of 1310 nm was observed., compared with the one-branched (or three-branched) chromophore, using comparable structure-unit-based concentrations. Optical stabilization capability of the dendritic chromophore was also observed. at this wavelength.

1-5. Optical power limiting and stabilization using novel two-photon absorbing liquid dye salt systems

Highly effective optical power limiting and stabilization performances have been achieved in a new type of two-photon absorbing medium. That is a liquid dye salt system, trans-4-[p-(N, N-dimethoxyethylamino)styryl]-N-3,6,9-trioxadecylpyridinium tetrafluoroborate (abbreviated as ASDPT), which features an unusually high molar concentration (~ 1 M) of two-photon absorbing chromophores and the capability of withstanding a higher pulsed laser power and energy. The nonlinear transmission property and output/input characteristics were studied based on a 1-cm long liquid dye salt sample by using nanosecond 1064-nm laser pulses with repetition rate variable from 1-10 Hz. A superior optical stabilization behavior of the studied material has been demonstrated; the relative fluctuation of the nanosecond laser pulses can be reduced more than two times by simply passing through this highly concentrated nonlinear absorbing medium.

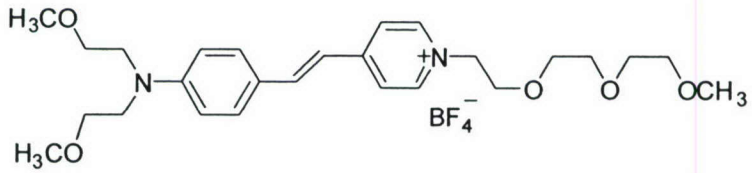

Fig. 6 Chemical structure a liquid stilbazolium dye (ASDPT) for optical limiting.

(Guang S. He, Qingdong Zheng, Paras N. Prasad, Roger Helgeson, Fred Wudl, Applied Optics, 2005, **44**, 3560-3564)

Highly effective optical power limiting and stabilization performances have been achieved in a new type of two-photon absorbing medium. That is a liquid dye salt system, trans-4-[p-(N, N-dimethoxyethylamino)styryl]-N-3,6,9-trioxadecylpyridinium tetrafluoroborate (abbreviated as ASDPT), which features an unusually high molar concentration (~ 1 M) of two-photon absorbing chromophores and the capability of withstanding a higher pulsed laser power and energy. The nonlinear transmission property and output/input characteristics were studied based on a 1-cm long liquid dye salt sample by using nanosecond 1064-nm laser pulses with repetition rate variable from 1 to10 Hz. A superior optical stabilization behavior of the studied material has been demonstrated; the relative fluctuation of the nanosecond laser pulses can be reduced more than two times by simply passing through this highly concentrated nonlinear absorbing medium.

The 1064-nm pulses from a Q-switched Nd:YAG laser system are suitable to be utilized for measuring the TPA property of the ASDPT sample. The beam size and the divergence angle of the lineally polarized laser beam used for this work were ~2 mm and ~1 mrad; the repetition rate of the laser pulses was variable from 1 to 10 Hz. The pulse duration was ~10 ns when a Pockels' cell was used as an electro-optic Q-switch element; however, this pulse duration was 13~15 ns with using a BDN dye-doped polymer sheet as the passive Q-switch element. The power (energy) stability of the output laser pulses is much better in case of using Pockels' cell than that with the BDN doped sheet.

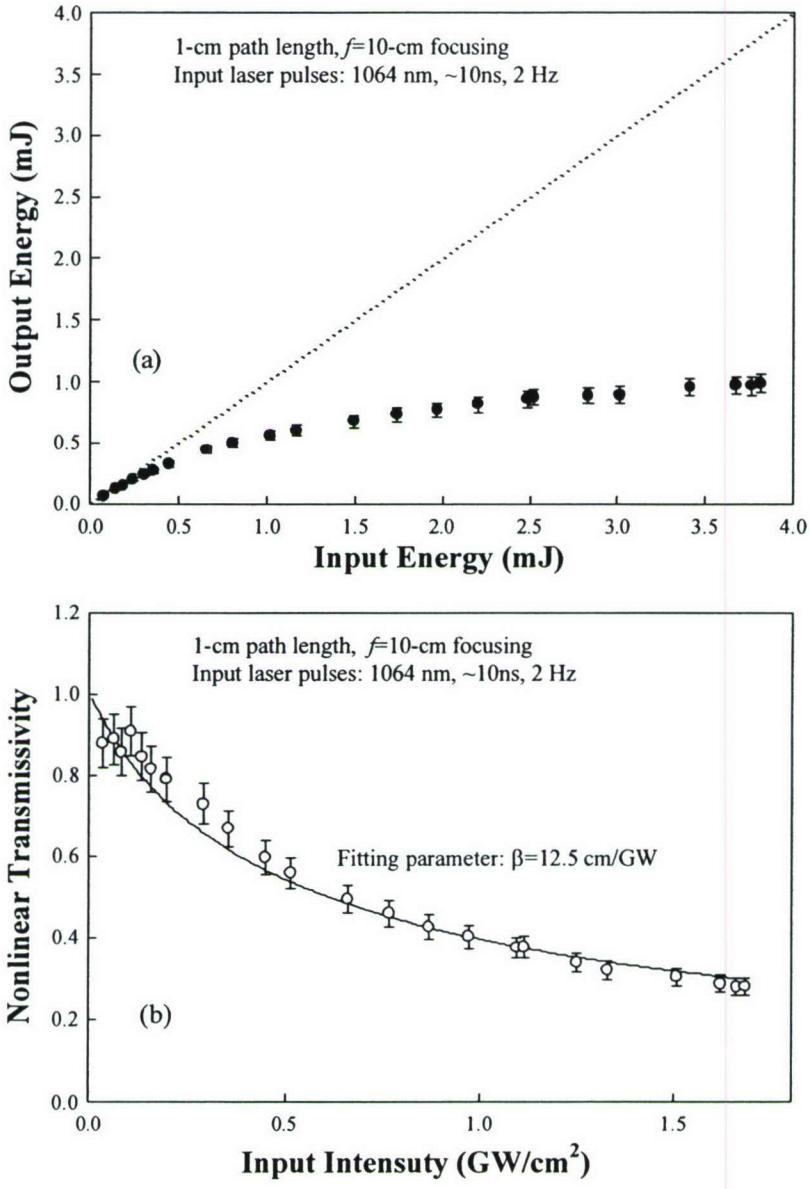

Fig. 7 Optical power limiting behavior of ASDPT sample: (a) Output/input curve, (b) Nonlinear transmission as a function of input laser intensity.

The measured output/input relationship for the 1064-nm laser pulses passing through a 1-cm path-length ASDPT sample of 1 M is shown in Fig. 7 (a). To do this measurement, the input laser beam from the Nd:YAG laser with a Pockels' cell as the Q-switch element, was focused via an f=10-cm lens onto the center of a 1-cm quartz cell containing the sample medium. In this case, the input pulse energy could be varied by rotating a polarization prism without changing the pulse shape and duration. Based on the data shown in Fig. 7 (a), the measured nonlinear

transmissivity as a function of the input laser intensity is shown in Fig. 7 (b), where the thick solid-line curve is a theoretical curve obtained by assuming an effective 2PA process with a best fitting parameter of 2PA coefficient β=12.5 cm/GW. From Fig. 7 (a) one can see that when the input energy increased from 0.18 to 3 mJ (17 times increase) the transmitted energy changed only from 0.15 to 0.89 mJ (5.9 times increase); thus it shows a typical optical limiting behavior.

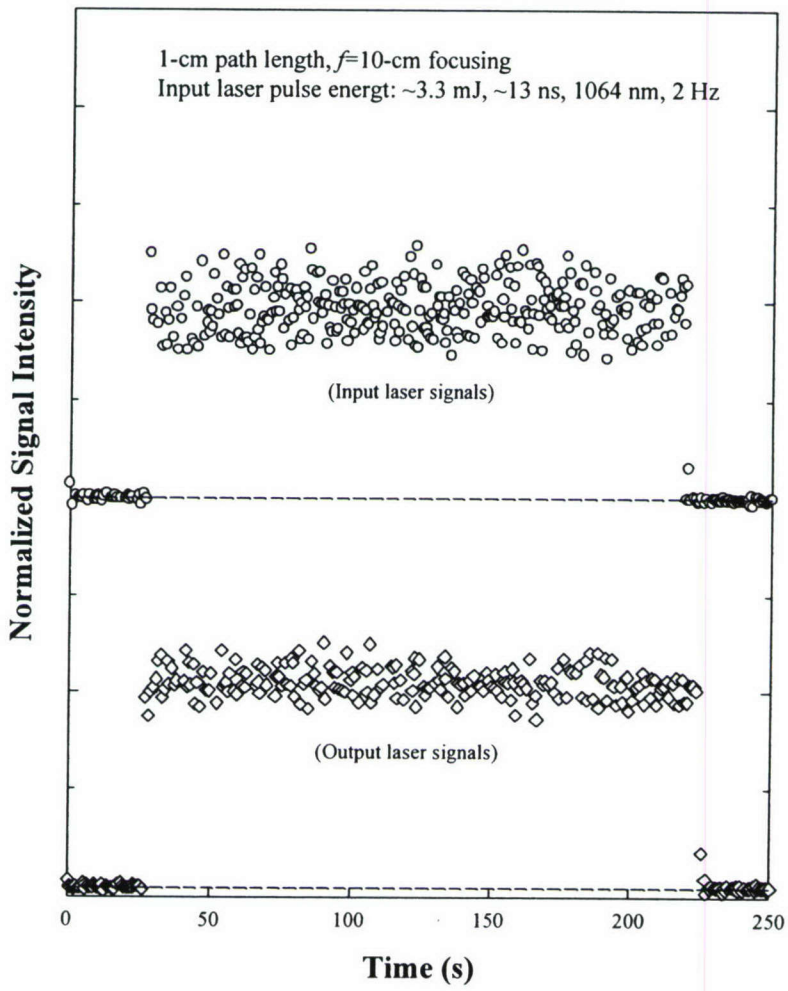

Fig. 8 Optical stabilization behavior of ASDPT sample: the fluctuation of the input laser pulses (upper trace) and the output laser pulses (lower trace).

On the other hand, from the viewpoint of many laser-based applications, such as optical telecommunication, optical fabrication, optical data storage and processing, a random intensity or power fluctuation is harmful. One of the best technical approaches to reduce such laser fluctuations is to make the laser beam simply passing through a two-photon absorbing nonlinear

medium. In Fig. 7 (a) we can see that if the input energy (or intensity) fluctuates within a range, for instance, from 3 to 3.7 mJ, the corresponding output will fluctuate within a much small range, i.e. from 0.89 to 0.97 mJ. For this specific example, the relative fluctuation range for the input is Δ_0=21%, while the corresponding output fluctuation range is Δ'=8.7%; this implies approximate 2.4 times improvement of the power stability.

To demonstrate the optical stabilization behavior of our two-photon absorbing medium, the 1064-nm laser pulses from the same Nd:YAG laser system, but now using a BDN-doped polymer sheet as the passive Q-switch element (working at repetition rate of 2 Hz), were focused and passed through a 1-cm long liquid dye salt sample. In this case, as mentioned before, the input laser energy exhibited a relatively larger fluctuation from pulse to pulse, which could be measured and recorded by using a gated integrator (Model 4422 from EG&G), working at gate width of 15 ns and in conjunction with a fast photodiode detector. In Fig. 8, the upper trace shows the temporal fluctuation of the input laser pulses around an average level of 3.3 mJ, whereas the lower trace shows fluctuation of the transmitted laser pulses at a different average level. In these cases each measured point corresponded to a single laser pulse with a repetition rate of 2 Hz. From Fig. 8, one can see that the relative fluctuation for the input pulsed signals was measured to be $\Delta_0 \approx \pm 25\%$, whereas the relative fluctuation for the output signals was $\Delta' \approx \pm 13\%$. Therefore, there is a two-fold reduction in the relative fluctuation for the transmitted laser pulses through the 1-cm long two-photon absorbing sample. The apparent reduction of the point number in the lower trace is due to overlapping of experimental points having very close values.

Another newly synthesized liquid dye salt system is *trans*-4-[4-(dihexylamino)styryl]-N-(2-{2-[2-(2-hydroxy-ethoxy)-ethoxy]-ethoxy}-ethyl)-pyridinium *p*-tosylate (abbreviated as ASEPT). The molecular structure of this system is shown in Fig. 9. In this structure, the long chain alkyl groups and the oligo(ethylene glycol) group are incorporated into the stilbazolium backbone for the purposes of decreasing its melting point and increasing its solubility in organic solvents. This liquid dye (ASEPT) was obtained through the Heck reaction between 4-bromo-N,N-dihexylaniline and 4-vinylpyridine, followed by quaternization with tetraethylene glycol mono(*p*-toluenesulfonate).

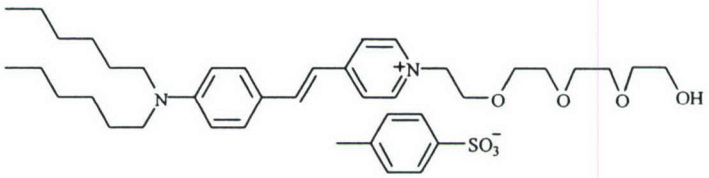

ASEPT

Fig. 9 Chemical structure of the liquid dye salt, ASEPT, for three-photon absorption based optical limiting

(Guang S. He, Qingdong Zheng, Changgui Lu, Paras N. Prasad, IEEE Journal of Quantum Electronics 2005, **41**, 1037-1043)

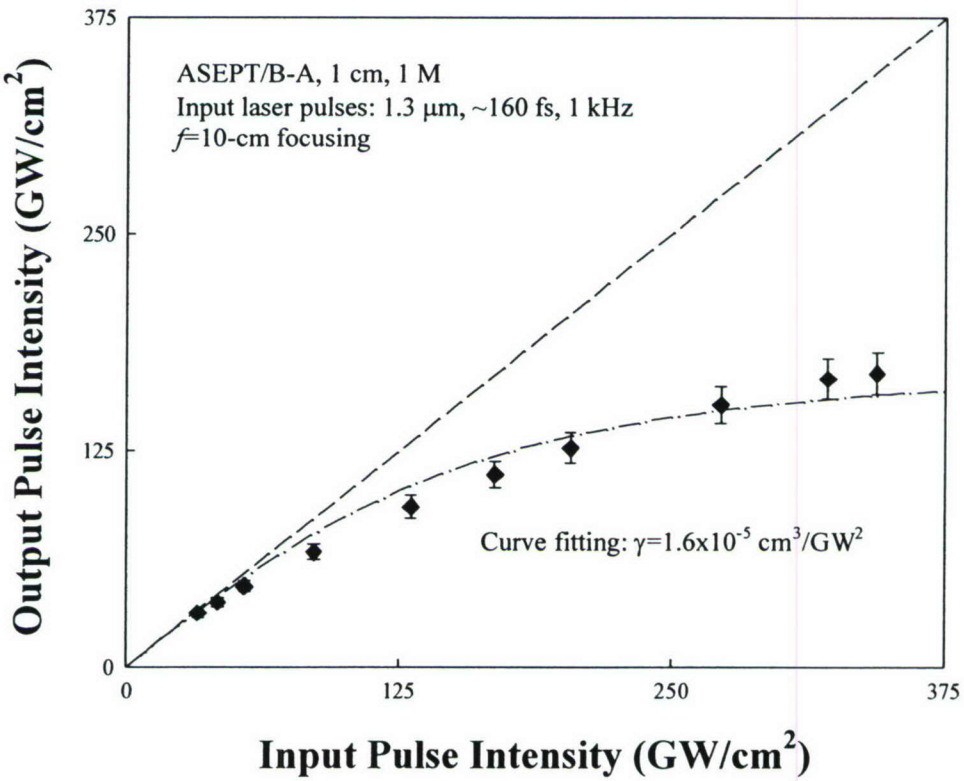

Fig. 10 Measured output intensity versus input intensity for the 1.3-μm laser pulses, the dash-dotted line represents the best fitting curve with a 3PA coefficient value of $\gamma=1.6\times10^{-5}$ cm^3/GW^2.

In our experiment, the 1.3-μm laser beam was generated from an optical parametric generator (OPG, a BBO crystal) pumped by the 775-nm laser pulses of ~160-fs duration and ~0.3 mrad divergence, which were from a Ti-sapphire oscillator/amplifier system (CPA-2010 from Clark-MXR) working at a repetition rate of 1 kHz. The precise wavelength and spectrum width could be determined by measuring the SHG spectrum of the 1.3-μm laser beam by passing through another BBO crystal. This 1.3-μm laser beam of ~2.5-mm size was focused by an f=10-cm lens onto the center of a quartz cuvette of either 1-cm or 2-cm path-length, filled with the same liquid dye sample of ~1 M concentration. For 3PA-based optical limiting performance, we have measured the nonlinear output/input relationship based on a 1-cm long sample, and the experimental results are shown in Fig. 10.

Figure 11 shows the relative intensity fluctuation of the input 1.3-μm laser pulses, as well as the output laser pulses passed through the 2-cm sample, recorded separately by the Boxcar with a gate width of 20 ns. The sampling rate of the Boxcar was 8 pulses per measured point. As the repetition rate of the input laser pulses was 1 kHz, the total measured points would be 7500 over an exposure period of 60 seconds. The average input pulse energy (or intensity) level was ~4 μJ (or ~ 500 GW/cm^2). From Fig. 11 one can see that after averaging over 8 pulses, the recorded relative fluctuation for the input pulses is $\Delta \approx \pm 33\%$, whereas the relative fluctuation for the transmitted laser pulses is reduced to $\Delta' \approx \pm 8\%$, correspondingly. Thus it is a strong experimental evidence of the drastic improvement of intensity stability of the laser pulses after passing through a three-photon absorbing medium.

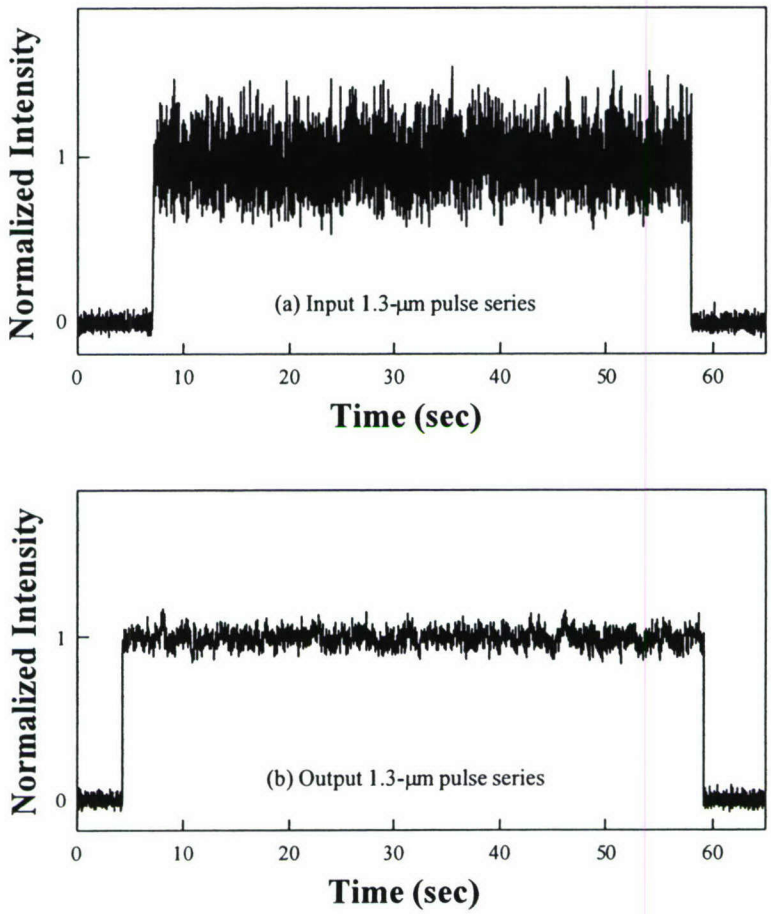

Fig. 11 (a) Normalized intensity-fluctuation profile of the input 1.3-μm and 1-kHz laser pulses; (b) Normalized intensity-fluctuation profile of the transmitted laser pulses after passing through a 2-cm 3PA medium.

Part II. Advanced materials for photorefractive and electro-optic devices

2-1. Efficient photosensitization and high optical gain in a novel quantum dot sensitized hybrid photorefractive nanocomposite at communication wavelength

The process of optical amplification associated with the asymmetric transfer of optical energy observed in the photorefractive two-beam coupling provides a means by which the polarization state of a signal beam or a phase-distorted information-carrying signal beam can be effectively "cleaned". A crucial issue for the application of polymeric photorefractive materials for this purpose is their potential ability to deliver high enough optical gain and display fast enough response at the optical wavelengths of commercial interest, such as 1.3 and 1.55 μm. A high-performance hybrid polymeric photorefractive nanocomposite (PVK:ECZ:DEANST:PbS) operating at the telecommunication wavelength of 1.34 μm has been developed. The photorefractive nanocomposite was sensitized with PbS nanocrystals synthesized via a hot colloidal route. Photoconductivity experiments confirmed and quantified the photocharge generation quantum efficiency of the nanocrystals (**Fig. 12**). The samples display greatly increased photocharge generation quantum efficiency, Φ, compared to previously reported results. Pronounced two-beam coupling effect at the operation wavelength was observed, leading to highest optical gains in hybrid photorefractive composites reported till date (**Fig. 13**). Temporal evolution of the photorefractive growth process was also studied. The dynamics of the grating build-up data permits a quantitative determination of the growth time constant associated with this PR composite under the given experimental conditions. A response time faster than other hybrid PR nanocomposites has been observed. This makes the material promising for all future applications in "image reconstruction".

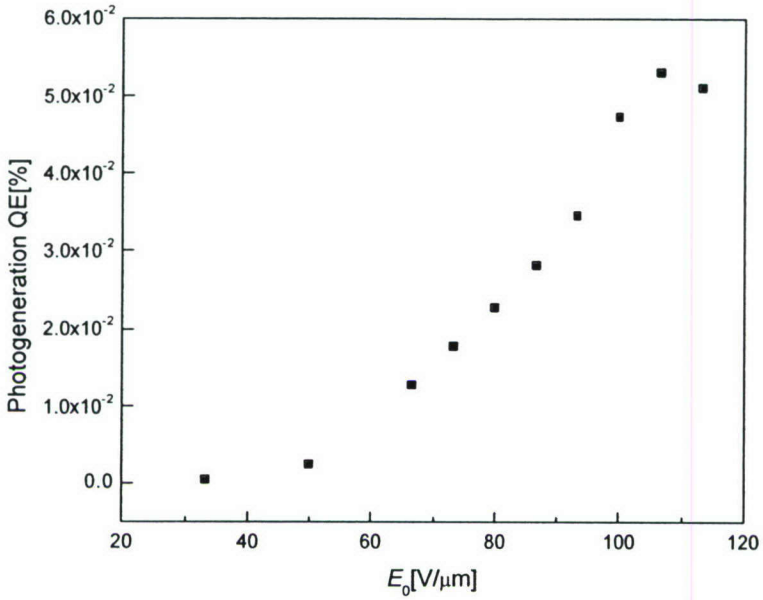

Fig. 12 Photocharge generation quantum efficiency, Φ, of the nanocomposite at 1.34 μm as a function of applied electric field, E_0.

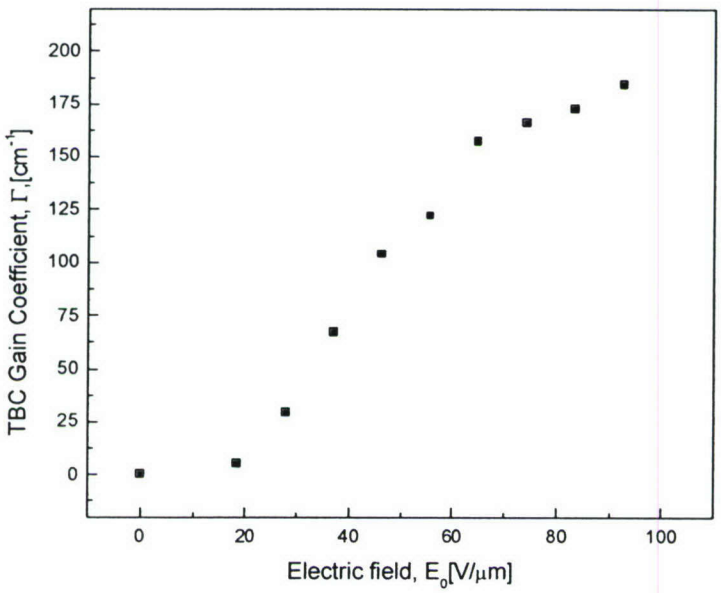

Fig. 13 Electric field dependence of the TBC gain coefficient Γ in the PVK:ECZ:DEANST:PbS nanocomposite at 1.34 μm. The highest gain recorded was 184.5 cm^{-1} at 92.6 V/μm.

2-2. New organically modified silica precursor systems for electro-optic devices

In order to achieve high performance electro-optic (EO) device, a series of new organically modified silica (ORMOSIL) precursors with high EO coefficient have been designed on the basis of semiempirical quantum chemical calculation on the molecular first hyperpolarizability (ß). The precursors are composed of triethoxysilyl group and organic EO chromophore unit whose generic structure contains electron-donating amino group, fluorene-based p-bridge, and a series of strong electron-acceptor. Some of them contain extra phenylenevinylene unit as a part of the p-bridge to enhance the molecular nonlinearity by increasing the conjugation length. In particular, fluorene was chosen due to its thermal-photochemical stability, enhanced planarity, and functionality to be modified laterally with bulky alkyl groups that can reduce electrostatic repulsion in the poled state as well as molecular aggregation in the high chromophore density film. The targeted molecules have been in preparation and one representative structure with an extremely high calculated ß value of 575×10^{-30} esu is shown below. Using the already prepared precursor, the optimization of factors for ORMOSIL glass fabrication is being investigated, which includes condition for the sol reaction, glass transition temperature, and degree of crosslinking before and after the poling process, etc.

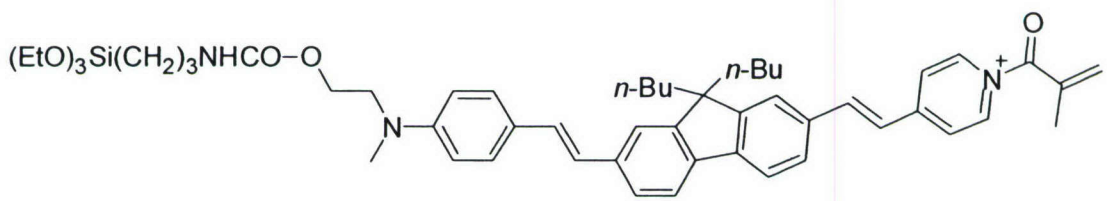

Fig. 14 New organically modified silica precursor systems for electro-optic devices

2-3. Efficient photoconductivity and photorefractivity at infrared wavelengths in hybrid nanocomposites

(A) High photoconductivity and narrow luminescence in solution-processed hybrid organic:inorganic nanocomposites at optical communication wavelengths

The photo-response of a polymer composite was extended to the 1.55 μm telecommunications band. Size tunable absorption of the semiconductor quantum dots enabled us to successfully sensitize the hybrid devices and tune their spectral response across the infrared range between 800 nm and 2 μm. The nanocomposites are photoactive at infrared wavelengths with narrow emission bands, tunable with the quantum dot sizes. The photoluminescence spans a wide spectral range in the infrared (**Fig. 15**). Efficient harvesting of infrared photo-generated carriers led to high photocurrents (**Fig. 16**). In particular, we observe for the first time, high photoconductive internal quantum efficiency (among the highest reported so far in this spectral range) in these hybrid devices at the technologically important wavelength of 1.55 μm (**Fig. 17**), achievable by low-power continuous-wave illumination, without the necessity of lock-in techniques.

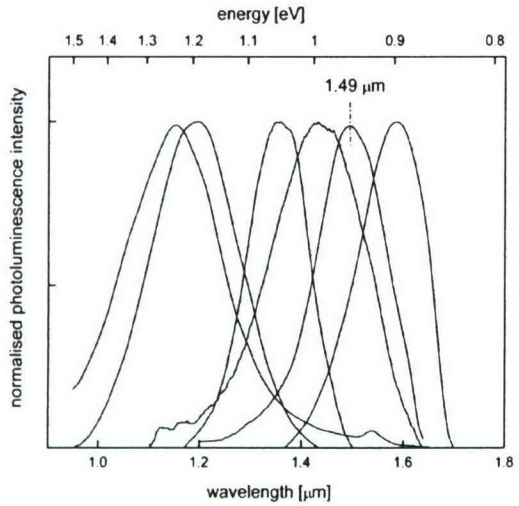

Fig. 15 Normalized room-temperature photoluminescence spectra of a series of polymer-NC composites, demonstrating size-tunable emission in the IR.

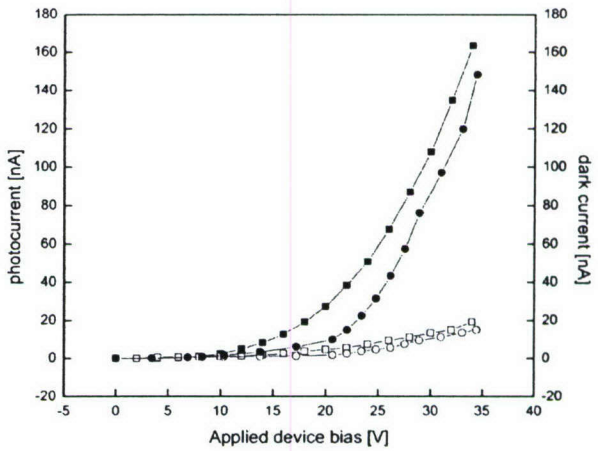

Fig. 16 Dark current (open circles and squares) and photocurrent (filled circles and squares) as a function of device bias, at excitation wavelengths of 1.34 μm (circles) and 1.55 μm

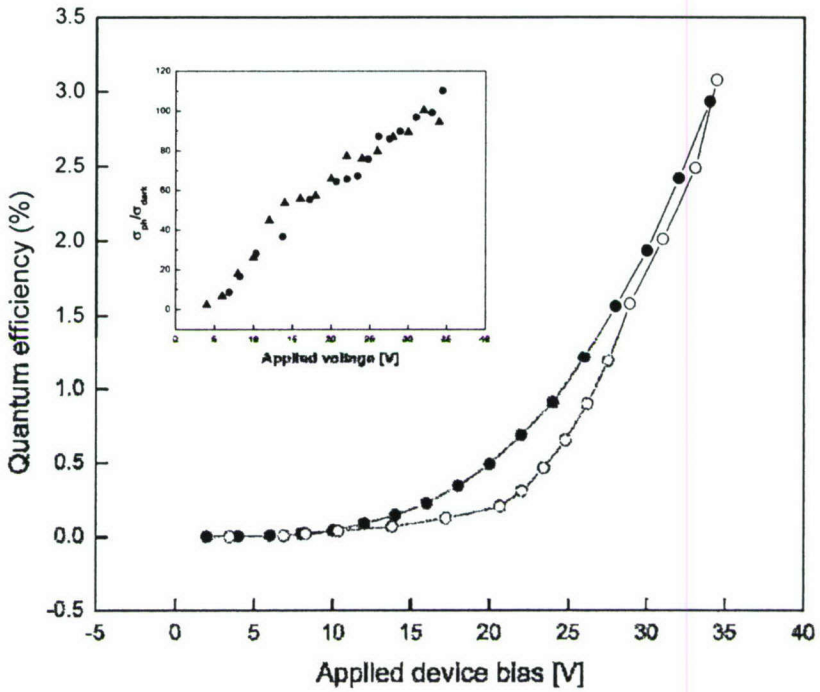

Fig. 17 Main Panel: photoconductive quantum efficiency as a function of device bias at excitation wavelengths of 1.34 μm (open circles) and 1.55 μm (filled circles). Inset: the ratio of photo- to dark conductivity for devices as a function of applied voltage, at excitation wavelengths of 1.34 μm (circles) and 1.55 μm (triangles).

(B) Polymer: quantum dot nanocomposite photorefractive device to open at 1550 nm optical communication wavelength.

Using colloidally-fabricated PbSe quantum dots (**Fig. 18**) photosensitization of a polymeric nanocomposite at the optical communication wavelength of 1550 nm is achieved (**Fig. 19**). Efficient generation of infrared photons lead to high photoconductivity and a significant figure of net gain co-efficient. A steady state diffraction efficiency of ~40% was obtained in the dynamic refractive-index gratings. The dynamics of the grating build-up was extracted by fitting a biexponential function to the temporal evolution of diffraction efficiency that is correlated to the growth of the internal space-charge field. The modulation amplitude of the refractive index is also computed from the diffraction efficiency data. The first observation of net optical gain and significant diffraction efficiency at this important wavelength, accomplished with low-power

continuous-wave laser beams, makes these hybrid nanocrystal-sensitized devices a potential choice for infrared imaging and optical communication applications.

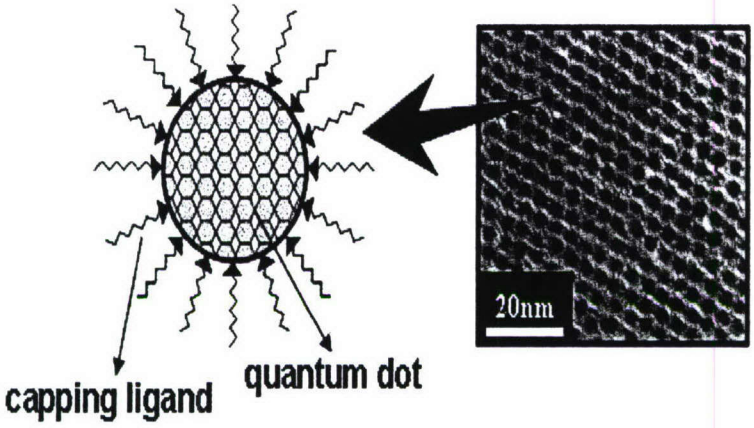

Fig. 18 Transmission electron icrograph (TEM) image of PbSe quantum dots ~5.2 nm size

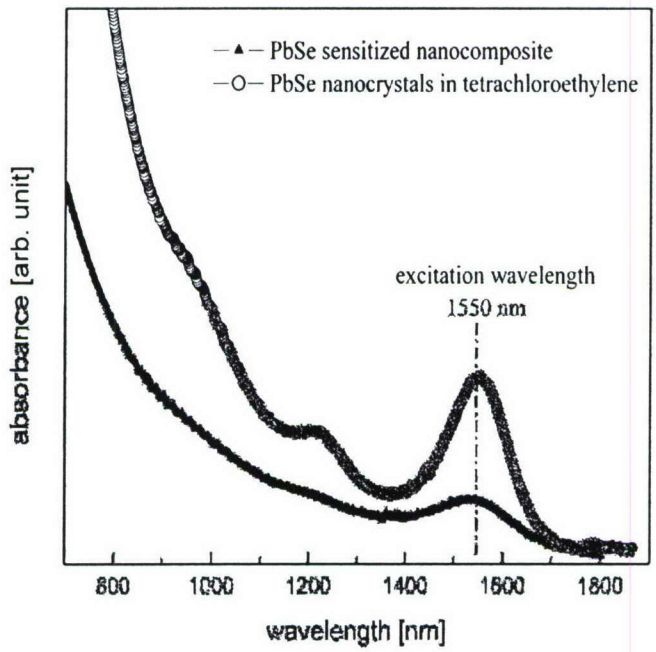

Fig. 19 Linear absorption spectrum of a batch of suitably size-tuned PbSe nanocrystal quantum dots in tetrachloroethylene and that of the composite system sensitized with PbSe.

Part III. Novel organic dyes for two-, three- and four-photon pumped frequency-upconversion lasing

3-1. Multi-photon pumped lasing dyes

Two-, three-, and four-photon pumped stimulated emission (cavityless lasing) properties of ten novel stibazolium dyes in solution phase have been comprehensively studied. These newly synthesized multi-photon active dye compounds have the same molecular backbone but differ either in their electron-donors or in their electron-acceptors, and can be utilized to effectively generate highly directional cavityless lasing in a quite broad visible spectral range (from 490 to 618 nm) under multi-photon pump conditions. The pump source was a powerful Ti:sapphire oscillator/amplifier system associated with an optical-parametric generator, which could specifically provide ~160-ps duration and ~775, 1320, and 1890-nm laser pulses for 2-, 3- and 4-photon excitation, respectively. The spectral, spatial, temporal, and efficiency properties for the multi-photon pumped lasing output from different dye solution samples have been studied. Based on the measured results, two salient features have been found: (1) the threshold pump energy values for 2-, 3-, and 4-photon pumped lasing were quite close (within factors 3~4); (2) these was an obvious wavelength difference (10~30 nm) between the forward and backward lasing under 3- and 4-photon pump conditions.

The molecular structures of the ten newly synthesized organic dye compounds with a simplified label (PRL-L#) are listed below. These stilbazolium dyes have the same molecular backbone but differ either in their electron-donors or in their electron-acceptors. Dialkylamino groups, alkyloxyl groups and hydroxyl group were chosen as electron donors. Various lasing wavelengths from these dyes can be obtained by changing the electron donating ability of the terminal groups on the stilbazolium backbone. Multi-photon pumped lasing with tunable wavelength can be achieved based on these dyes in solutions. At the same time, different electron donors or acceptors may influence dye interactions with a surrounding medium (solvent), which may affect their multi-photon pumped lasing properties. Structure/lasing properties investigation of this class of dye molecules may help researchers to design and synthesize the future multi-photon active dye materials.

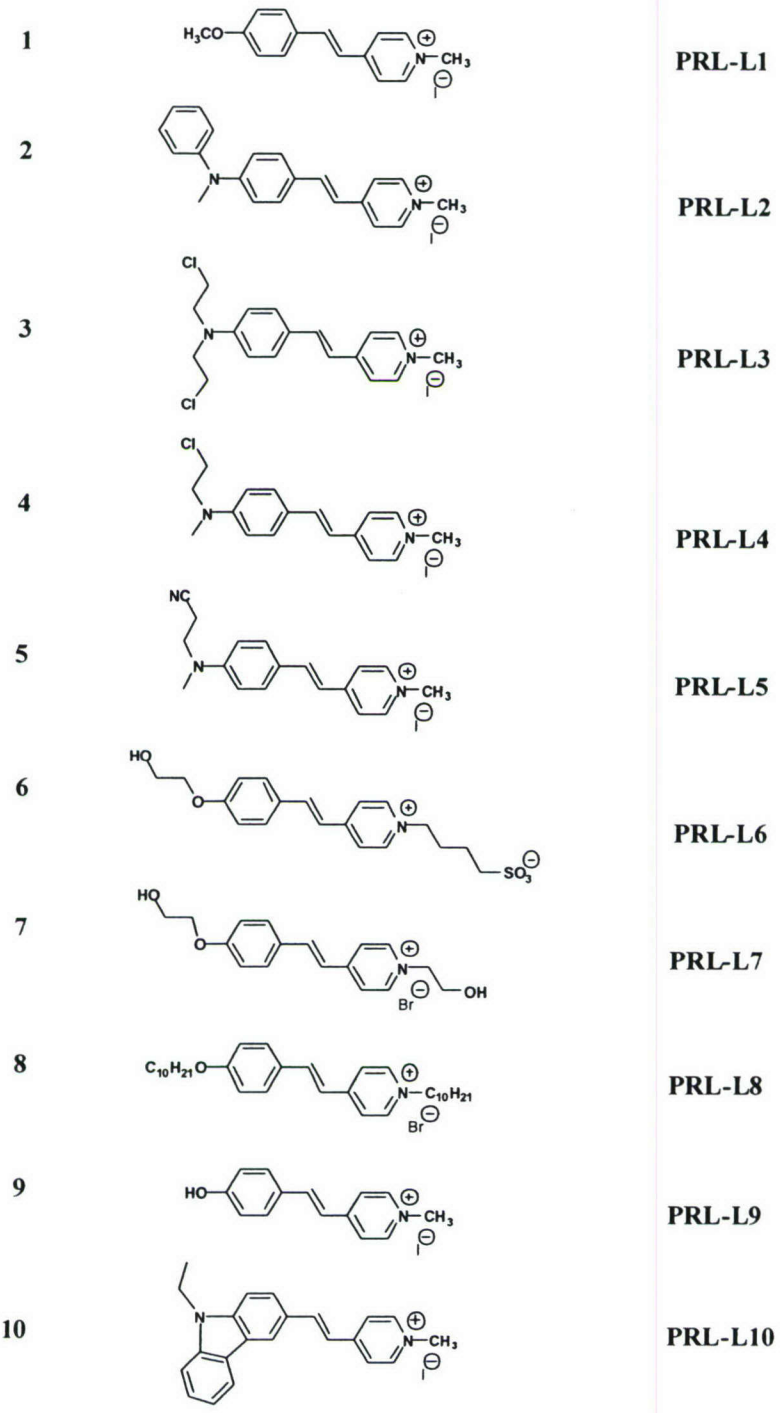

Fig. 20 Molecular structures of ten newly synthesized stilbazolium dye compounds.

(Guang S. He, Tzu-Chau Lin, Sung-Jae Chung, Qingdong Zheng, Changgui Lu, Yiping Cui, Paras N. Prasad, J. e Opt. Soc. Am. B 2005, **22**, 2219-2228.)

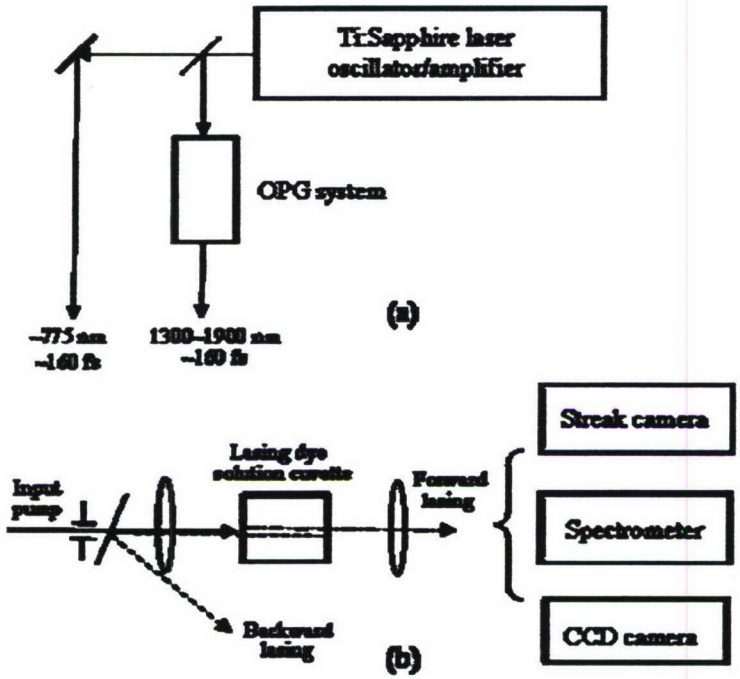

Fig. 21 Pump laser sources (a) and optical setup (b) for multi-photon pumped lasing experiments.

3-2. Multi-photon pumped lasing properties

As schematically shown in Fig. 21, the pump beam of ~4 mm diameter from the Ti:sapphire laser or from the OPG was focused by an f=10-cm (or 5-cm) lens on the center of a 1-cm path-length quartz cuvette filled with our dye solution (mostly of concentration 0.02 M). The input pump intensity or energy can be varied either through a rotated prism polarizer or a variable neutral-density (ND) filter-set without changing the pump pulse duration (~0.16 ps). Once the pump intensity inside the gain medium was higher than a certain threshold value, a highly directional and visible coherent emission could be observed in both the forward and backward directions based on the single-pass stimulated amplification of original spontaneous seed signals propagating inside a population-inversion dye solution. It was found that the forward and backward stimulated emission properties did not change when the incident angle of the pump beam varied from 5 to 15°. The experimental results of near-field and far-field measurements of the output stimulated emission from our dye solution samples show that the spatial structures for the input pump laser beam and the output stimulated emission beam are basically the same. On the basis of this fact and also for simplicity, we sometimes use the term "cavityless lasing" (or simply "lasing") instead of the term "stimulated emission" or "amplified

spontaneous emission" (ASE). It is known that in many reported experimental studies of one- or two-photon excited stimulated emission, the observed ASE signals only showed the spectral narrowing but no spatial directionality. The experimental results of two-photon (2P), three-photon (3P), and four-photon (4P) pumped lasing studies are summarized in Table 1.

Table 1. Multi-photon pumped cavityless lasing and fluorescence parameters for ten novel dye solutions.

Dye	Solvent Concentration (1-cm path length)	Fluorescence lifetime τ^* (ps)	Lasing threshold* (μJ)	Forward lasing wavelength# (nm)	Backward lasing wavelength# (nm)	Net lasing efficiency (%)
PRL-L1	DMSO/0.02 M EG/0.04 M	65 (2P) 85 (3P) 70 (2P) 100 (3P)	0.46 (2P) 1.5 (3P)	495 (2P) 494 (3P)		
PRL-L2	DMSO/0.02 M	11 (2P)	no (2P) 1.5 (3P)	 607 (3P)		
PRL-L3	DMSO/0.02 M	620 (2P) 680 (3P)	1.2 (2P) 0.88 (3P) 2 (4P)	605 (2P) 579 (3P) 580 (4P)	606 (2P) 598 (3P) 580 (4P)	4.5 (2P)[a] 13 (3P)[a] 0.12 (4P)[b]
PRL-L4	DMSO/0.02 M	200 (2P) 225(3P)	2.0 (2P) 0.88 (3P)	618 (2P) 594 (3P)	620 (2P) 612 (3P)	
PRL-L5	DMSO/0.02 M	243 (2P) 285 (3P)	1.2 (2P) 0.66 (3P) 2 (4P)	616 (2P) 593 (3P) 593 (4P)	618 (2P) 611 (3P)	13 (3P)[a]
PRL-L6	EG/0.01 M	110 (2P) 155 (3P)	3.2 (2P) 4.1 (3P)	502 (2P) 496 (3P)		
PRL-L7	EG/0.04 M	80 (2P) 110 (3P)	1.9 (2P) 1.8 (3P)	498 (2P) 490 (3P)		
PRL-L8	DMSO/0.02 M	110 (2P) 118 (3P)	0.57 (2P) no (3P)	511 (2P)		
PRL-L9	DMSO/0.02 M	92 (2P) 115 (3P)	0.46 (2P) no (3P)	516 (2P)	519 (2P)	
PRL-L10	DMSO/0.02 M	1200 (3P)	0.95 (2P) 1.2 (3P) 3.9 (4P)	595 (2P) 564 (3P) 565 (4P)	596 (2P) 594 (3P)	3.6 (3P)[c]
(Note)			(f=10 cm)			(f=5 cm)

*

Uncertainty: ±10%
Uncertainty: ±1 nm
a Concentration: 0.08 M
b Concentration: 0.02 M
c Concentration: 0.1 M

As am example, Fig. 22 shows the 4P-pumped lasing structures from a PRL-L3 solution in DMSO-d_6, pumped by ~1890-nm and ~160-fs laser pulses. The remarkable feature in Fig. 22 is that the forward lasing wavelength is obviously shorter than the backward lasing wavelength. This apparently unexpected effect can be well explained by using our physical model considering several different dynamic processes.

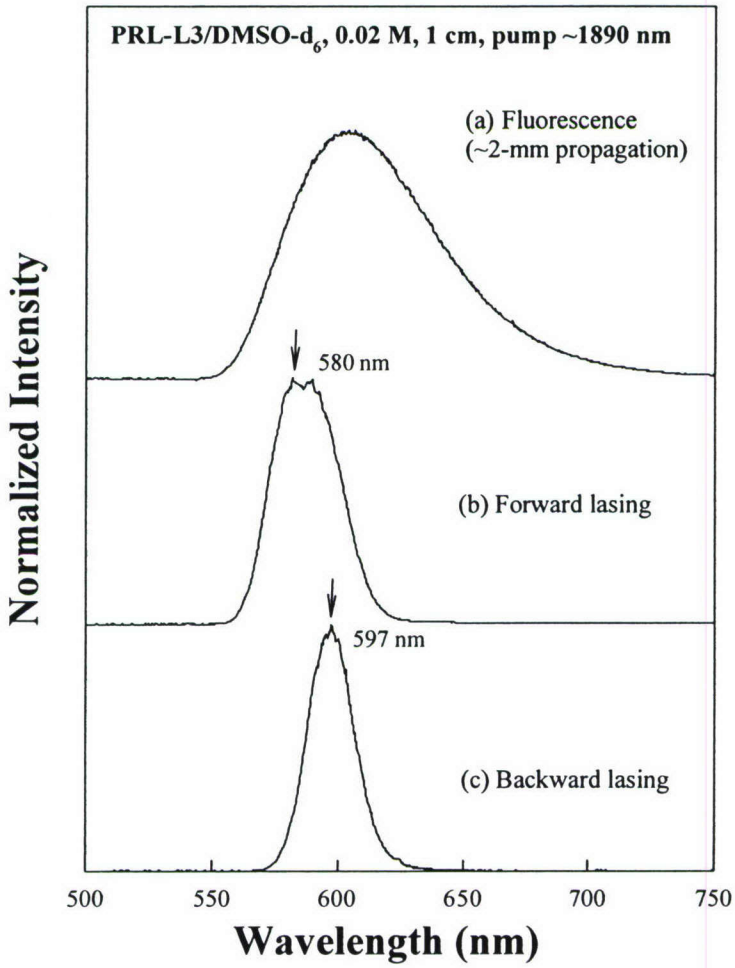

Fig. 22 Measured spectra of (a) the four-photon excited fluorescence, and (b) & (c) the forward and backward 4PP lasing from PRL-L3/DMSO-d_6 solution at the pump level of ~4.8 μJ.

Finally, under 4P pumped condition, the output lasing energy as a function of the input pulse energy is shown in Fig. 23 for PRL-L3 dye solution of 0.02 M concentration. From Fig. 23 we can see that at the input level of 4.8 μJ, the forward 4PP lasing output is 5.7 nJ, therefore the

overall lasing efficiency is ?~ 0.12 %. No effort was made to achieve a higher lasing efficiency by increasing the dye concentration.

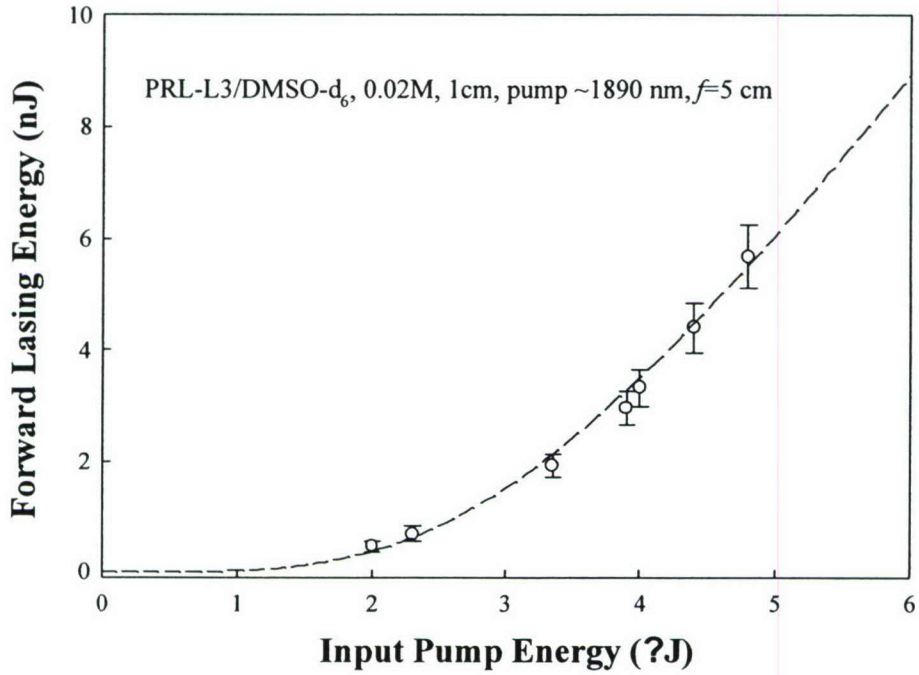

Fig. 23 Measured output/input characteristic curve for 4PP lasing from PRL-L3/DMSO-d_6 solution.

In summary, we have achieved 2P-, 3P-, and 4P-pumped stimulated emission (cavityless lasing) in a series of newly synthesized stilbazolium dyes in their solution phase, using ultra-short intense pump pulses of wavelength ~775, ~1320, and 1890 nm, respectively. The spectral, spatial, temporal properties and output/input characteristics have been comprehensively studied. There are two salient features that have not been reported. First, it is found that under our experimental conditions, the measured pump energy threshold values for 2PP-, 3PP-, and 4PP lasing in these tested solution samples are quite close (within the same order of magnitude). Second, for 3PP and 4PP lasing, there is an obvious (17-30 nm) wavelength difference between the forward and backward stimulated emission from the same dye solution, provided that the pump level is considerably higher than the threshold value.

Part IV. A new-type stimulated Rayleigh-Bragg scattering generated in a novel two-photon absorbing dye solution

4-1. Stimulated Rayleigh-Bragg scattering in a two-photon absorbing dye solution

Recently we have discovered a new type of stimulated scattering effect that is a two-photon excitation enhanced backward stimulated scattering in a nonlinearly absorbing dye solution. This stimulated scattering shows no frequency shift and therefore is different from most of other known stimulated scattering processes. Comparing to all other known light stimulated scattering effects, including stimulated Raman scattering (SRS), stimulated Brillouin scattering (SBS), stimulated Kerr scattering (SKS) and stimulated thermal Rayleigh scattering (STRS), this new effect, namely *stimulated Rayleigh-Bragg scattering* (SRBS), exhibits the following three favorable features: (1) there is no frequency-shift between the input pump beam and the backward stimulated scattering beam, (2) the pump threshold requirement is lower, and (3) the spectral linewidth requirement of the pump beam is lower. All these three features are highly desirable for many stimulated scattering-based applications, such as optical phase-conjugation technique which can automatically remove aberration and disturbance influences from the propagation or gain media, frequency-degenerate optical feedback and amplification, and optical power limiting and stabilization.

The scattering medium, specifically employed for this experimental demonstration, is a two-photon absorbing dye solution: PRL802 in tetrahydrofuran (THF of spectroscopic grade). This dye is one of a series of novel two-photon absorbing chromophores synthesized by our group for 2PA-based optical limiting and frequency-upconversion lasing purposes. The chemical structure of the dye molecule and linear absorption spectra for two solutions with different concentration and pass-lengths are shown in Fig. 24, from which one can see that there is no linear absorption for PRL 802/THF in the spectral range from 520 to 875 nm.

The pump laser beam of 532-nm was provided by a Q-switched and frequency-doubled Nd:YAG laser system that utilized either an electro-optical Pockels as the active Q-switching element or a saturable BDN dye-doped acetate sheet (from Kodak) as the passive switching element. In these two cases, the output spectral line-width was ~0.8 cm^{-1} for the former and 0.08 cm^{-1} for the latter. The other measured parameters of the 532-nm pump laser beam were: ~10-ns pulse duration, ~3.5-mm beam size (before focusing), ~1-mrad divergence angle, and 5-Hz repetition rate. The input 532-nm laser beam was focused via an f=10-cm lens onto the center

of a 1-cm long quartz cuvette filled with the PRL802/THF solution of 0.01 M concentration. The incident angle of the input pump beam on the liquid cell was around 10-15° to avoid the reflection influence from the two optical windows of this cuvette.

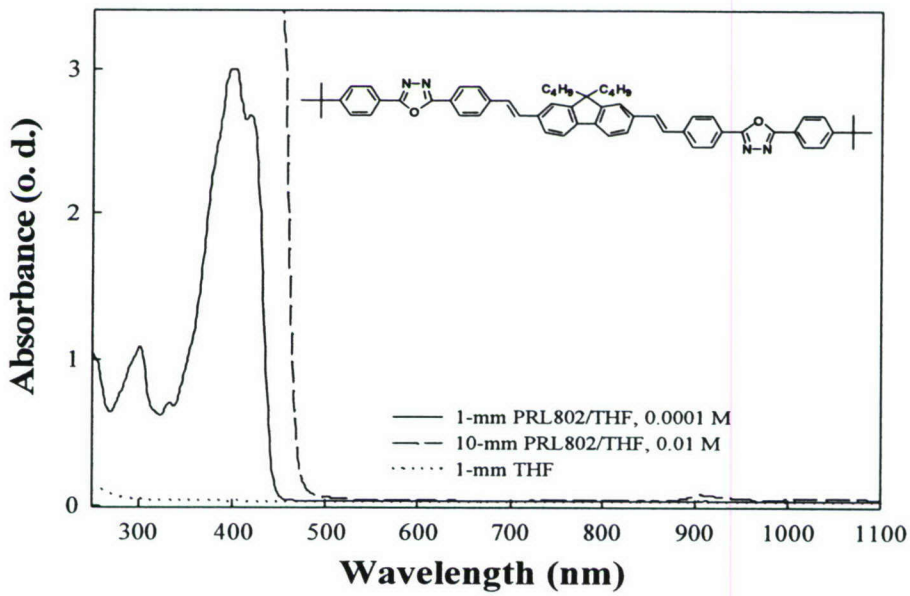

Fig. 24 Molecular structure and linear absorption spectrum of PRL-802.
(Guang S. He, Tzu-Chau Lin; Paras N. Prasad, Optics Express, 2004, **12**, 5952-5961)

It was found that once the input laser energy (or intensity) exceeded a certain threshold value (~60 μJ or ~40 MW/cm^2), a highly directional and backward stimulated scattering beam could be observed. To identify the spectral property of the observed stimulated scattering, a F-P interferometer of 1-cm spacing was used in conjunction with an f=50-cm lens and a CCD camera. This combined spectral recording system exhibited a spectral resolution of 0.025 cm^{-1}, which was calibrated by using an ultra-narrow-line (≤0.005 cm^{-1}) 532-nm laser beam from an injection seeded Nd:YAG laser system (PRO230-10, from Spectra-Physics).

Finally, we have measured the nonlinear transmission of the input pump beam passing through the sample solution as well as the backward stimulated scattering energy as a function of the input laser energy. The results are shown in Fig. 25 (a) and (b), respectively. In both cases the change in the input pulse energy was controlled by rotating a polarization prism without changing the pulse duration. From Fig. 25 (a) we can see that when the input energy (or

intensity) level is lower than the threshold value, the attenuation of the pump beam can be well fitted with a 2PA process. However, once the pump level is higher than the threshold, there is an additional pump energy loss which is transferred to the backward stimulated scattering, as shown in Fig. 25 (b). Moreover, it should be noted that under our experimental conditions the above mentioned pump threshold value (~60 μJ) is considerably lower than that for SBS and SRS in a pure solvent (THF) sample of spectroscopic grade under the same experimental conditions.

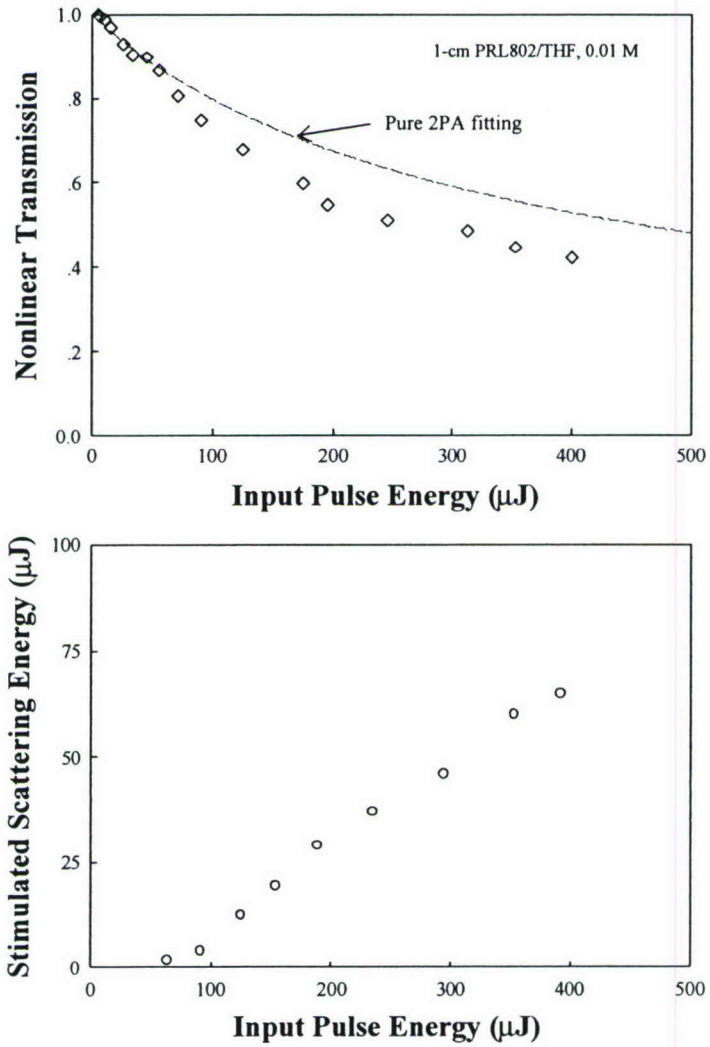

Fig. 25 (a) Measured nonlinear transmission of 532-nm pump pulses, the dashed-line curve is the best fit with a 2PA coefficient of β=9.46 cm/GW; (b) Measured output stimulated scattering energy vs. input pump energy.

4-2. Significance of stimulated Rayleigh-Bragg scattering studies

For an input intense pulsed laser beam, when its intensity is greater than a certain threshold level, the backward stimulated scattering will take place and cause nonlinear attenuation of the output laser beam. In this sense, the mechanism of backward stimulated Rayleigh-Bragg scattering in multi-photon absorbing media will enhance the optical power limiting performance of these materials.

On the other hand, this new type of stimulated scattering effect in multi-photon active media may attract enough attention and general interest for the research community of physics, because of its unique features, broad material selections, and application potentials. As an example, for developing future X-ray laser devices, a special optical feedback element is essentially needed, as the conventional optical mirrors do not work for X-ray beams. In this case, a specially selected multi-photon active medium (crystal or optical fiber), which is capable to generate backward stimulated Rayleigh-Bragg scattering, can play the role of a phase-conjugate "cavity mirror" to ensure a positive feedback for cavity lasing. As the Rayleigh scattering cross-section is inversely proportional to the fourth power of the wavelength, the discussed stimulated scattering effect may be much easily realized in X-ray spectral ranges.

Personnel Supported:

Paras N. Prasad, PhD. PI, summer salary
Guang Sheng He, Senior Research Scientist
QingDong Zheng, Post-Doctoral Associate
Sehoon Kim, Post-Doctoral Associate
Purnendu Dutta, MD. Research Specialist
Alexander Kachynski, Post-Doctoral Associate
Ander Kuzmin, Post-Doctoral Associate
Koichi Baba, Post-Doctoral Associate
Gen Xu, Technician
Kaushik Roy Choudhury, Graduate Student
Hoon Hi Lee, Graduate Student
Marjorie Weber, Administrative Assistant
Judith Garven, Administrative Assistant
Theresa Skurzewski, Administrative Assistant

Publications

1. Q. Zheng, G. S. He and P. N. Prasad, "Novel two-photon-absorbing, 1,10-phenanthroline-containing π-conjugated chromophores and their nickel(II) chelated complexes with quenched emissions," *J. Mater. Chem.* **15**, 579-587 (2005).
2. T.-C. Lin, G. S. He, P. N. Prasad, and L.-S. Tan, "Degenerate Nonlinear Absorption and Optical Power Limiting Properties of Asymmetrically Substituted Stilbenoid Chromophores," *J. Mater. Chem.* **14**, 982-991 (2004).
3. R. Kapoor, N. Kaur, E. T. Nishanth, S. W. Halvorsen, E. J. Bergey, and P. N. Prasad, "Detection of Trophic Factor Activated Signaling Molecules in Cells by a Compact Fiber-Optic Sensor," *Biosensors & Bioelectronics* **20**, 345-349 (2004).
4. D. W. Brusmiche, J. M. Serin, J. M. J. Frechet, G. S. He, T.-S. Lin, and P. N. Prasad, "Fluorescence Resonance Energy Transfer in Novel Multi-Photon Absorbing Dendritic Structures," *J. Phys. Chem.* B **108**, 8592-8600 (2004).
5. S. M. Dunham, H. E. Pudavar, P. N. Prasad, and M. K. Stachowiak, "Cellular Signaling and Protein-Protein Interactions Studied Using Fluorescence Recovery After Photobleaching," *J. Phys. Chem.* B **108**, 10540-10546 (2004).
6. T. Y. Ohulchanskyy, D. J. Donnelly, M. R. Detty, and P. N. Prasad, "Heteroatom Substitution Induced Changes in Excited State Photophysics and Singlet Oxygen Generation in Chalcogenoxanthylium Dyes: Effect of Sulfur and Selenium Substitutions," *J. Phys. Chem.* B **108**, 8668-8672 (2004).
7. P. N. Prasad, "Polymer Science and Technology for New Generation Photonics and Biophotonics," Current Opinion in Solid State and Materials Science **8**, 11-19 (2004).
8. P. P. Markowicz, M. Samoc, J. Carne, P. N. Prasad, A. Pucci, and G. Ruggeri,"Modified Z-scan Techniques for Investigations of Nonlinear Chiroptical Effects," *Opt. Express* **12**, 15209 (2004).
9. G. S. He and P. N. Prasad, "Two-Photon Absorption Induced Stimulated Rayleigh-Bragg Scattering," *SPIE Proceedings*, Vol. **5646**, 37-43 (2005).
10. K. R. Choudhury, Y. Sahoo, S. Jang, and P. N. Prasad, "Efficient Photosensitization and High Optical Gain in a Novel Quantum Dot Sensitized Hybrid Photorefractive Nanocomposite at Communication Wavelength," *Adv. Funct. Mater.* **15**, 751-756 (2005).

11. Q. Zheng, G. S. He, and P. N. Prasad, "Novel Two-Photon Absorbing, 1,10-phenanthroline Containing D-conjugated Chromophores and Their Nickel(II) Chelated Complexes with Quenched Emissions," *J. Mat. Chem.* **15**, 579-587 (2005).
12. G. S. He, Q. Zheng, P. N. Prasad, R. Helgeson, and F. Wudl, "Nonlinear Optical Stabilization of 1064-nm Laser Pulses with a Novel Two-Photon Absorbing Liquid-Dye Salt System," *Appl. Opt.* **44**, 3560-3564 (2005).
13. P. P. Markowicz, G. S. He, and P.P. Prasad, "Direct Four-Photon Excitation of Amplified Spontaneous Emission in a Nonlinear Organic Chromophore," *Opt. Lett.* **30**, 1369-1371 (2005).
14. G. S. He, Q. Zheng, C. Lu, and P. N. Prasad, "Two-and Three-Photon Absorption Based Optical Limiting and Stabilization Using a Liquid Dye," *IEEE J. Quantum Electron.* **41** 1037-1043 (2005).
15. G. S. He, C. Lu, Q. Zheng, P. N. Prasad, P. Zosom, R. W. Boyd, and M. Samoc, "Stimulated Rayleigh-Bragg Scattering in Two-Photon Absorbing Media," *Phys. Rev.* A **71**, 063810 (2005) .
16. A. Baev, P. N. Prasad, and M. Samoc, "Ab Initio Studies of Two-Photon Absorption of Some Stilbenoid Chromophores," *J. Chem. Phys.* **122**, 224309/1-224309/6 (2005)
17. G. S. He, T-C. Lin, S-J. Chung, Q. Zheng, C. Lu, Y. Cui, and P. N. Prasad, "Two-, Three-, and Four-Photon Pumped Stimulated Emission Properties of Ten Stilbazolium-Dyes Solutions," *J. Opt. Soc. Amer.* B **22**, 2219-2228 (2005).
18. K. R. Choudhury, Y. Sahoo, T. Y. Ohulchansky, and P. N. Prasad, "Ultra Efficient Photoconductive Device at Mid-IR Wavelengths from Quantum Dot-Polymer Nanocomposites," *Appl. Phys. Lett.* **87**, 073110-1-073110-3, (2005).
19. A. V. Kachynski, A. N. Kuzmin, H. E. Pudavar, and P. N. Prasad, "Three-Dimensional Confocal Thermal Imaging Using Anti-Stokes Luminescence," *Appl. Phys. Lett.* **87** , 023901/1-023901/3 (2005).
20. Q. Zheng, G. S. He, and P. N. Prasad, "A p-Conjugated Dendritic Nano-Sized Chromophore with Enhanced Two-Photon Absorption," *Chem. Mater*, **17**, 6004-6011 (2005).

21. K. R. Choudhury, Y. Sahoo, and P. N. Prasad, "Hybrid Quantum Dot-Polymer Nanocomposite for Infrared Photorefractivity at the Optical Communication Wavelength of 1,550 nm," *Adv Mater.* **17**, 2877-2881 (2005).
22. Q. Zheng, G. S. He, P. N. Prasad, "π-Conjugated Dendritic Nanosized Chromophore with Enhanced Two-Photon Absorption," *Chem. Mater.* **17**, 6004-6011 (2005)
23. Q. Zheng, G. S. He, C. Lu, and P. N. Prasad, "Synthesis, two- and three-photon absorption, and optical limiting properties of fluorene-containing ferrocene derivatives," *J. Mater. Chem.*, **15**, 3488-3493 (2005).
24. S. Kim, Q. Zheng, G. S. He, D. J. Bharali, H. E. Pudavar, A. Baev, and P. N. Prasad, "Aggregation-Enhanced Fluorescence and Two-Photon Absorption in Nanoaggregates of a Novel 9,10-*Bis*[4-(4`-amino styryl)styryl] anthrolene Derivatives," *Adv. Func. Mater.* 16, 2317-2323 (2006).
25. Q. Zheng, G. S. He, A. Baev, and P. N. Prasad, "Experimental and quantum chemical studies of cooperative enhancement of three-photon absorption, optical limiting, and stabilization behaviors in multibranched and dendritic structures," *J. Phys. Chem.* B **110**, 14604-14610 (2006).
26. G. S. He, C. Lu, Q. Zheng, A. Baev, M. Samoc, and P. N. Prasad,"Asymmetric Properties Between the Forward and Backward Stimulated Emission Generated by Ultrafast Three- and Four-photon Excitation," Phys. Rev.A , 033815/1-033815/10 (2006).
27. P. A. Padmawar, T. Canteenwala, S. Verma, L.-S. Tan, G. S. He, P. N. Prasad and L. Y. Chiang, "Synthesis of C60-diphenylaminofluorene Dyads with Two-Photon Absorbing Characteristics," Chem. Mater. 18(17), 4065-4074. (2006)
28. G. S. He, Q. Zheng, P. N. Prasad, J. Grote, and F. Hopkins, "Infrared Two-Photon Excited Visible Lasing from a DNA-surfactant-chromophore Complex," Opt. Lett. 31(3), 359-361.(2006)
29. M. A. Oar, W. R. Dichtel, J. M. Serin, J. M. J. Fréchet, J. E. Rogers, J. E. Slagle, P. A. Fleitz, L.-S. Tan, T. Y. Ohulchanskyy, and P. N. Prasad "Light-Harvesting Chromophores with Metallated Porphyrin Cores for Tuned Photosensitization of Singlet Oxygen via Two-Photon Excited FRET", , Chem. Mater. 18(16) 3682-3692 (2006).

30. T. C. Lin, G. S. He, Q. Zheng, and P. N. Prasad, "Degenerate two-/three-photon absorption and optical power-limiting properties in femtosecond regime of a multi-branched chromophore," *J. Mater. Chem.* **16**(25), 2490-2498 (2006).
31. P. A. Padmawar, J. E. Rogers, G. S. He, L. Y. Chiang, L-S. Tan, T. Canteenwala, Q. Zheng, J. E. Slagle, D. G. McLean, P. A. Fleitz, and P. N. Prasad, "Large cross-section enhancement and intramolecular energy transfer upon multiphoton absorption of hindered diphenylaminofluorene-C_{60} dyads and triads," *Chem. Mater.* **18**, 4065-4074 (2006).
32. G. S. He, Q. Zheng, and P. N. Prasad, "Stimulated Rayleigh-Bragg scattering in a three-photon absorbing medium and its phase-conjugation property," *J. Opt. Soc. Am.* B 24, 2007 (in press).
30. G. S. He, Q. Zheng, A. Baev, and P. N. Prasad, "Saturation of three-photon absorption upon strong and ultrafast infrared laser excitation," *J. Appl. Phys.* **101**, 2007 (in press).